

# Effect of Load Pattern on Cold-formed Steel Wall Plate System

Adeline Ng Ling Ying, Hii Wei Hui and Mei Chee Chiang

**Abstract**—This paper presents the behavior and the modes of failure of cold-formed steel wall plate system subjected to different load position. An experimental investigation was conducted on a full scale wall plate system. Load was applied at the mid span of the wall plate and the system was tested to failure. The behavior of the system was observed and the data collected was used to calibrate a numerical model for parametric study. To study the effect of load position on the system, a concentrate force was applied at different positions on the wall plate. Different failure modes and capacities were observed as the load moved away from the mid span of the wall plate. The system had the highest capacity when load was applied at the support and the lowest ultimate capacity when load was applied at the mid span of the wall plate.

**Keywords**—load pattern, cold-formed steel, wall plate, failure mode, ultimate capacity

## I. Introduction

The use of cold-formed steel (CFS) structures in the construction industry in Malaysia is still limited as compared to advanced countries like Australia, United Kingdom and United States of America. They were seldom used in the main building structures but were commonly used in building roof trusses, replacing wood trusses. CFS trusses are noncombustible and termite proof thus, are well suited for the local tropical rainforest climate.

To maintain the standard of CFS trusses constructions, a specification was published by the Malaysian Public Work Department as a guide to the industry. It is a requirement to use wall plate in all CFS roof truss construction. The minimum section size of the wall plate and the spacing of the anchors were stated in the specification. However, the details of the connections were not provided and the system has not been tested for its overall behavior. Literature review showed that existing studies done mainly on the individual members and the interaction between members and the effect of load pattern were not taken into consideration. Experimental tests done by Ng and Hii (2014) showed that the capacity of the wall plate system was affected by the interaction of the individual members. Besides that, different failure modes were observed. Thus, it is the aim of this study to investigate the effect of load pattern on the system.

A wall plate system consists of connecting plates (U-brackets and L-plates), lipped C-channel and screwed and bolted connections which were designed to resist vertical and horizontal forces. These elements were designed individually according to current design standards. In this study, the Australia/New Zealand design standards were referred (Standards Australia and Standards New Zealand, 2005).

## II. Experimental Investigation

A laboratory test setup as shown in Fig. 1 was designed to study the behaviour of the wall plate system under an uplift force.



Figure 1. Laboratory test setup

### A. Test specimens

Locally available thin walled lipped C-channels were used as wall plates for this study. The section had a nominal web width ( $w$ ) of 100 mm, flange width ( $f$ ) of 50 mm, lip length ( $l$ ) of 15 mm and plate thickness ( $t$ ) of 1.2 mm as shown in Fig. 2. The C-channel was labelled as C10012 where the first letter, C refers to C-channel, the next three digits, 100 refers to the web width ( $w$ ) and the last two digits, 12 refers to the thickness ( $t$ ) of the section.

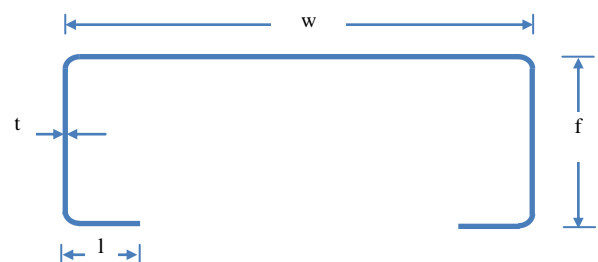


Figure 2. Nominal dimensions of lipped C-channel

Adeline Ng Ling Ying  
Swinburne University of Technology Sarawak  
Malaysia

Hii Wei Hui  
Swinburne University of Technology Sarawak  
Malaysia

Mei Chee Chiang  
EcoSteel Sdn. Bhd.  
Malaysia

The shapes and the nominal dimensions of the U-bracket and L-plate are shown in Fig. 3. The nominal widths of the L-plates and U-brackets were 50 mm. All the plates were fabricated according to the tolerance given in AS1391 (2007).

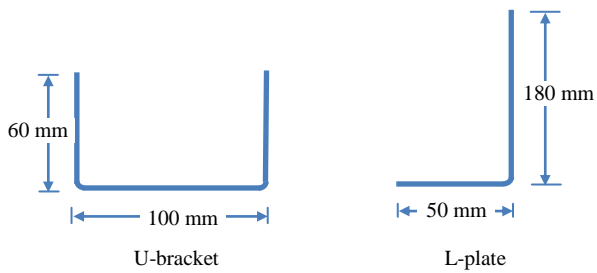


Figure 3. Nominal dimensions of connecting plates

The fasteners used in this study were grade 8.8 M16 bolts and ASTeks RedPoint self-drilling, self-tapping screws. The bolts were used to anchor the U-brackets to the supports and to connect the L-brackets to the loading rig whereas the screws were used to connect the U-brackets to the C-channel and the C-channel to the L-plates as shown in Fig. 4.

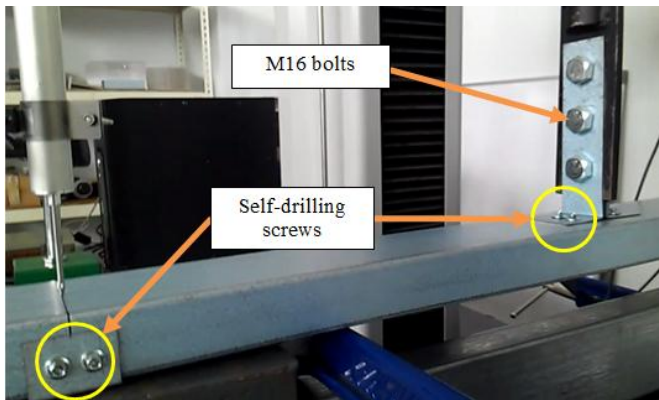


Figure 4. Positions of fasteners on the wall plate system

### B. Material Properties

High strength aluminium zinc coated grade G550 AZ150 steel sheets were used to fabricate the lipped C-channel and the connecting plates. The yield strength for the material used was determined using tensile coupon test in accordance to the Australian standard, AS1391 (2007). It was found that the steel sheet has yield strength,  $\sigma_y$  of 585MPa and tensile strength,  $\sigma_u$  of 587MPa. The ductility of the material,  $\epsilon$  is 9%.

### C. Test Setup

The laboratory test setup was designed according to the recommendation of the specification. The C-channel was supported at 1.0 m span and loaded with a concentrated force in between its supports. Force was applied using a universal testing machine (UTM) and was increased gradually at a constant rate of 10 mm/min. The schematic view of the test setup is shown in Fig. 5. At least 2 sets of sample were tested. If the result obtained for a sample fall beyond a 10% limit, the result for that particular sample was omitted and a third test was conducted to replace the inconsistent data.

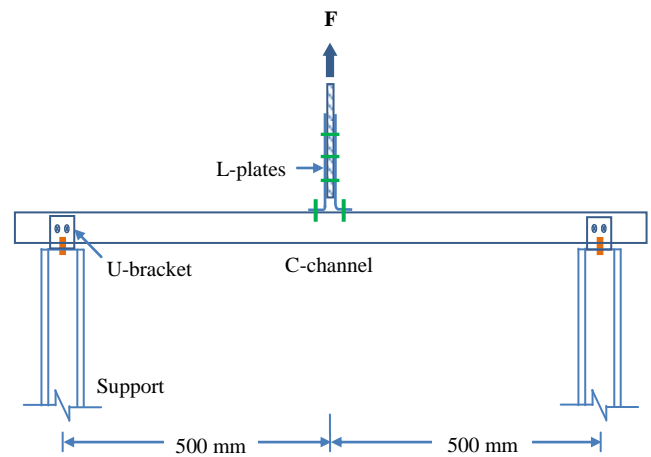


Figure 5. Schematic view of test setup

## III. Experimental Observation

It was observed that the connecting plates and the C-channel deformed elastically in the direction of the force when load was applied. Then, yielding occurred in the connecting plates where yield lines were formed along the edge of the connecting bolt and screw heads. The C-channel continued to bend further as loading continued. After a while, the screws connecting the L-plates began to tilt. Upon reaching the ultimate load, the C-channel buckled at the centre of the section. The deformed sample is shown in Fig. 6.



Figure 6. Deformation of the wall plate system

The force displacement data collected from the experimental tests were plotted in force displacement graphs to facilitate analysis. The ultimate capacity of the system was taken as the force at the peak of the force displacement graph and the yield capacity was taken at the point where there was a change in stiffness (Ng and Mei, 2010) as shown in Fig. 7. The yield capacity for this system was 2.6 kN and the ultimate capacity was 8.02 kN.

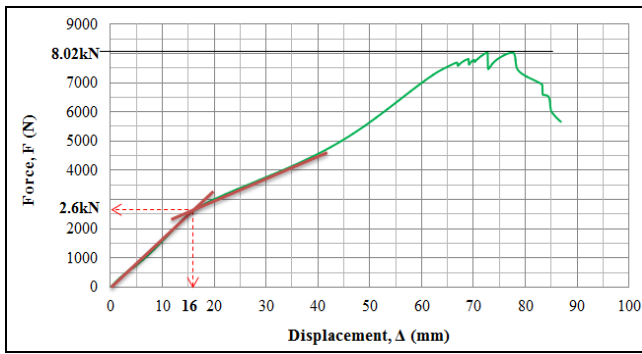


Figure 7. Force displacement curve of wall plate system

## IV. Numerical Investigation

The Finite Element Analysis (FEA) Software that was used in this study was ANSYS 15. As the models for this study were complicated, a separate CAD system called the SolidWorks was used to model the geometry components and imported into ANSYS. The model comprised of 4 main components; a lipped C-channel, a pair of U-brackets, a pair of L-plates and screws. The components were built according to the actual dimensions measured in the laboratory test.

### A. Geometric Models

In order to reduce analysis time and computing space, the geometric model was simplified. The model was halved in the longitudinal axis as it was symmetrical. The simplified model is shown in Fig. 8.

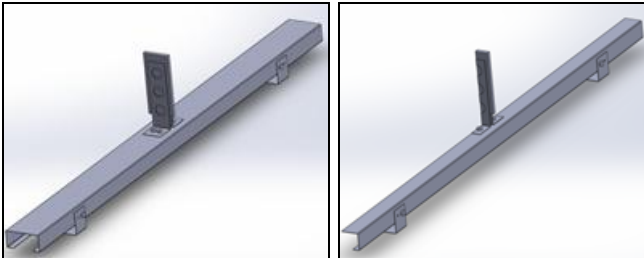


Figure 8. Halving the model

Besides that, the screw component was built using two cylinders instead of actual screw with threads. The ANSYS's body-body beam connector feature was used where bolt thread contact was replaced with a cylindrical joint (Jandric, 2014). The beam connector was used at three locations on the model as shown in Fig. 9. In the first location, the beam connector was used as a pin. This was because no failure was observed at the outermost screws of the connection in the laboratory tests. In the second location, a 0.4 mm thick beam connector was inserted in between the U-bracket and the C-channel to allow tilting to occur. In the third location, it was set such that pull out occur when the capacity of the screwed connection was reached. Although the model was simplified, it was tested to ensure that it was able to simulate the actual behavior of the wall plate system.

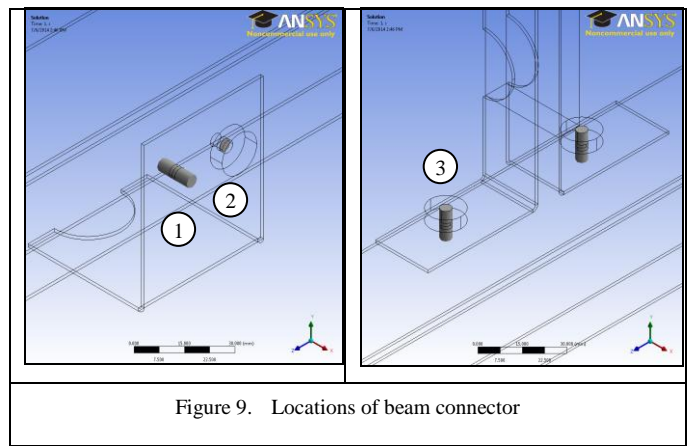


Figure 9. Locations of beam connector

### B. Boundary Condition

To simulate the wall plate system which was held down by a bolt at the U-bracket, the edge around the bolt holes of the U-bracket were applied with fixed supports. Besides that, a frictionless support was applied along the surface of the halved cross-section in the longitudinal direction. This frictionless support allowed the model to move vertically but was restraint in the horizontal direction.

In the laboratory testing, an incremental uplift force was applied at the mid span of the wall plate through the loading rig. In the numerical model, the behavior of the wall plate system was studied by applying an incremental displacement at the loading plate. Displacement control was used instead of force control so that post buckling behavior of the system may be observed. An incremental displacement was applied at the top surface of the plate connecting the L-plates.

### C. Material Properties

The material type chosen from the material library was structural steel. It had basic material properties such as steel density and modulus of elasticity. The existing yield and ultimate strengths were updated according to the data obtained from tensile coupon tests. Besides that, the properties of screw were also updated according to the data obtained from the product catalogue.

### D. Mesh and Quality Control

In this study, the multizone sweep meshing was used. This advanced sweeping approach supports multiple source and target selection. It also allowed for sizing and mapped controls. Hexa mesh type was used to mesh the C-channel and the screw components whereas Prism mesh was used in the U-brackets and L-plates as in Fig. 10. The Prism mesh produced more accurate results but it used more nodes and computing time.

To ensure the quality of the mesh, the skewness of the mesh elements was examined. The sizes of the elements were adjusted so that majority of the elements were within 0.25 skewness value (ANSYS, 2015). Besides that, the distribution of the mesh on the model was also examined. The mesh was ensured to be symmetrically distributed. According to the failure modes observed in the laboratory test, a denser mesh was applied at areas which were more susceptible to failure such as around the screw holes and the



connecting plates. These areas were more highly stressed as compared to the rest of the model.

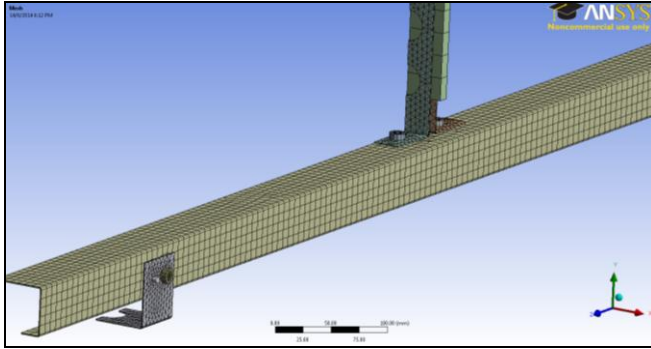


Figure 10. Meshing of model

### E. Contacts

Two types of contacts were used in this model; bonded and frictional contacts. Bonded contact was used to prevent relative movement between the surfaces. In this model, it was applied in between the L-plate and loading plate contact surfaces and at the screw head and L-plate contact surfaces. Frictional contact was applied with a friction coefficient value 0.2 taking into consideration of the materials' surface condition (Beardmore, 2013). Frictional contact was applied at surfaces in between the screws and the plates and the plates to the C-channel.

### F. Model Calibration

In order to validate the numerical model, the data retrieved from the FEA was plotted in a force displacement graph and compared with the experimental curve as shown in Fig. 11. The ultimate capacity of the model was also determined and compared with the experimental capacity. The ultimate capacity was 7.96 kN, only 1% different from the experimental capacity. Besides that, the behavior of the model was observed and its failure modes were recorded.

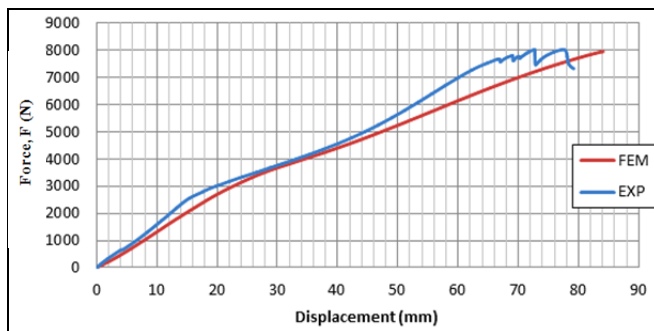


Figure 11. FEA and experimental force displacement curves

### G. Numerical Observation

The simulation of the FE model showed that the model behaved similar to the experimental model. It was observed that the model lifted up when the loading plate moved upward. The connecting plates then yielded and geometric hardening occurred as the plates were pulled in tension. At the same time the C-channel bent and finally buckling occurred at the mid span of the C-channel. The deformation of the finite element model, FEM is shown in Fig. 12.

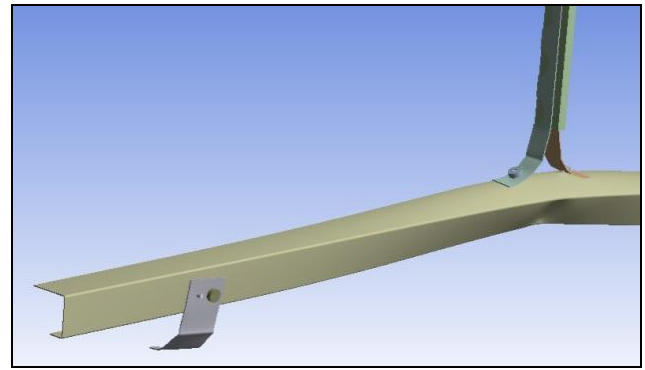


Figure 12. Deformation of FEM

### H. Parametric Study

In the parametric study, load was applied at different positions of the wall plate by shifting the L-plates position from the mid span of the C-channel as in Fig. 13. Load was applied at every 100 mm interval from the mid span of the C-channel to the support.

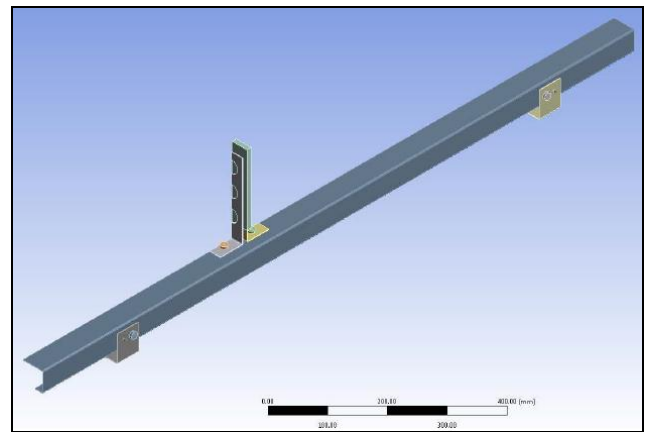


Figure 13. Shifted position of L-plates on the wall plate

It was observed that the behavior of the wall plate system changed when the applied loading shifted from the mid span of the C-channel. When load was applied within a 100 mm distance from the mid span of the C-channel, it was observed that failure began with the yielding of connecting plates followed by the buckling of the C-channel. The deformations of the connecting plates are shown in Fig. 14. However, when load was applied 200 mm to 300 mm away from the mid span of the C-channel, bearing failure was also observed at the screwed connections between the U-bracket and the C-channel before buckling occur. And when load was applied 400 mm away from the mid span of the C-channel and on top of the U-bracket support, failure began with yielding of connecting plates followed by pull out of screws at the L-plates connections as in Fig. 15. No buckling was observed in the C-channel. Observations on these models showed that yielding of connecting plates will occur regardless of the position of load on the wall plate.

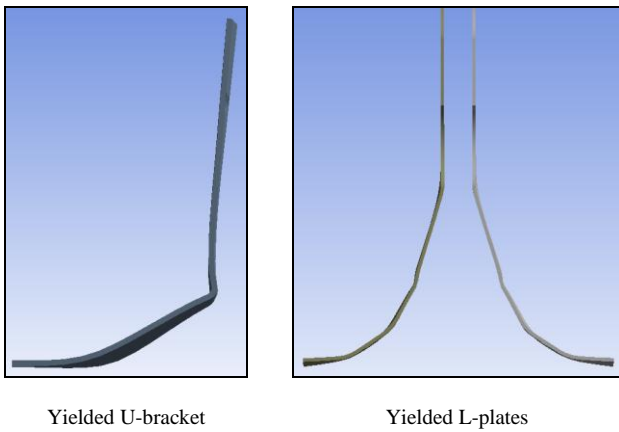


Figure 14. Deformation of connecting plates



Figure 15. Screws pull out at the L-plates to C-channel connections

The ultimate capacity of the wall plate system subjected to different load positions was plotted in a force position graph shown in Fig. 16. It was found that the system had the lowest capacity when load was applied at the mid span of the wall plate. The capacity gradually increased as load shifted from the mid span of the wall plate to the support. The system had the highest capacity when load was applied at the support. This was because the behavior of the wall plate system changed with the position of load as discussed earlier. Besides that, it was observed that the system was stiffer when load was applied nearer to the support.

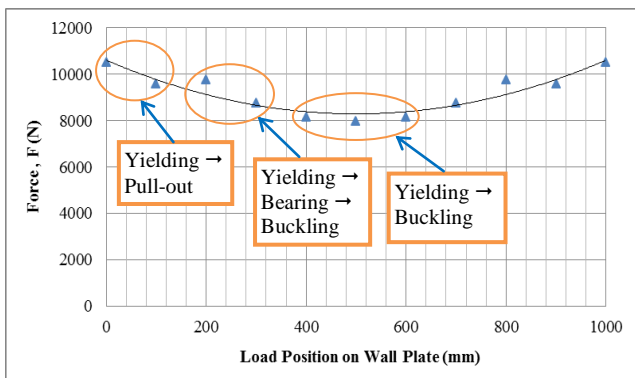


Figure 16. Ultimate load of wall plate system at different load positions

## v. Conclusions

The experimental investigation to study the behavior of wall plate system was successfully conducted. A FEM was successfully calibrated in the ANSYS finite element software. The numerical model behaved similar to the experimental model. Failure began with the yielding of connecting plates followed by buckling of C-channel. The ultimate capacity of the models was also within a 10% limit. The numerical model was used to determine the effect of load position on the system. It was found that the ultimate capacity and behavior of the wall plate system changed with the position of applied loading. The system had the lowest capacity when load was applied at the mid span of the wall plate. The capacity gradually increased when load was applied nearer to the supports. Instead of buckling in the C-channel, screws pull out were observed at the connections between the L-plates and C-channel. Nevertheless, all the connecting plates were yielded before the ultimate failure regardless of the position of the load.

## Acknowledgment

The research described in this paper was financially supported by the Swinburne Sarawak Research Grant.

## References

- [1] Standards Australia and Standards New Zealand, AS/NZS 4600: Cold-formed Steel Structures, 2005.
- [2] Standards Australia, AS 1391: Metallic materials: tensile testing at ambient temperature, 2007.
- [3] A.L.Y. Ng and W.H. Hii, "Experimental investigation on cold-formed steel wall plate system," International Journal of Civil, Architectural, Structural and Construction Engineering, Vol:8 No:4, pg.467-473, 2014.
- [4] A.L.Y. Ng and C.C. Mei, "The Behaviour of Cold-formed Steel Anchor Plate Subjected to Pure Axial Tension Force", Steel & Composite Structures, p.304-306, 2010.
- [5] D. Jandric, "An overview of methods for modelling bolts in ANSYS V15," ANSYS Regional Conference, Chicago, 2014. <http://www.ansys.com/staticassets/ansys/staticassets/conference/download/chicago-comprehensive-guide-to-bolt-modeling-in-ansys-15-0.pdf>
- [6] ANSYS , "Determining mesh quality," Chapter 20.2, Ansys Notes, SAS IP, Inc., 2015. [https://www.sharcnet.ca/Software/Ansys/16.0/en-us/help/tgd\\_usr/tgd\\_user\\_report\\_quality.html](https://www.sharcnet.ca/Software/Ansys/16.0/en-us/help/tgd_usr/tgd_user_report_quality.html)
- [7] R. Beardmore, "Friction coefficients," Roytech, 2013. [http://www.roytech.co.uk/Useful\\_Tables/Tribology/co\\_of\\_frict.htm](http://www.roytech.co.uk/Useful_Tables/Tribology/co_of_frict.htm)